Original Paper

Pathobiology

Pathobiology 2009;76:303–314
DOI: 10.1159/000245896

Received: March 26, 2009
Accepted after revision: June 24, 2009

Regulation of 5-Aminolevulinic Acid-Mediated Protoporphyrin IX Accumulation in Human Urothelial Carcinomas

Keiji Inoue[a] Takashi Karashima[a] Masayuki Kamada[a] Taro Shuin[a] Atsushi Kurabayashi[b] Mutsuo Furihata[b] Hirofumi Fujita[c] Kozo Utsumi[c] Junzo Sasaki[c]

Departments of [a]Urology and [b]Pathology, Kochi Medical School, Nankoku, and [c]Department of Cytology and Histology, Okayama University Graduate School of Medicine, Dentistry and Pharmaceutical Sciences, Okayama, Japan

Key Words
Urothelial lesions · Cancer · Flow cytometry · Photodynamic diagnosis · 5-Aminolevulinic acid · Protoporphyrin IX

Abstract
Purpose: The purpose of this study was to clarify the regulatory mechanism of protoporphyrin IX (PpIX) synthesis mediated by 5-aminolevulinic acid (ALA) in human urothelial carcinoma (UC), leading to improved accuracy in photodynamic diagnosis and therapy using ALA. ***Experimental Design:*** PpIX accumulation in cultured UC cells after incubation for 1–5 h with 0.5–5 mM ALA was analyzed by fluorescence analysis using fluorescence microscopy and flow cytometry technique. ***Results:*** PpIX fluorescence mediated by ALA was increased, and the intensity of PpIX fluorescence was time-dependently increased in UC cells compared to noncancerous cells. The distribution of endogenous PpIX fluorescence primarily coincided with mitochondria, and then increased at a specific perinuclear region in the cells during the time of incubation. The ALA-mediated PpIX synthesis in UC cells was suppressed by β-alanine, an inhibitor of β-transporters of cell membrane, and carbonyl cyanide *p*-trifluoromethoxyphenyl hydrazone, an uncoupler of mitochondrial oxidative phosphorylation. In contrast, the ALA-mediated PpIX accumulation was increased by deferoxamine, an iron chelator, manganese and nitric oxide, which is contributed to PpIX metabolism by inhibiting ferrochelatase activity, generated by a nitric oxide-generating reagent NOC-18. As observed above, ALA-mediated PpIX synthesis in human UC cells was regulated by the process of ALA uptake, ALA conversion to PpIX and metabolism of accumulated PpIX to heme. ***Conclusions:*** This shows that the suppression of ferrochelatase increased PpIX accumulation in UC cells using small amount of ALA, thus leading to an improved clinical practicability of photodynamic diagnosis and therapy.

Introduction

Photodynamic diagnosis (PDD) and therapy (PDT) using 5-aminolevulinic acid (ALA) as a photosensitizer is clinically recognized as an effective procedure of detection and treatment for various cancers such as brain tumor, skin tumor and esophageal tumor [1–3]. Recently, PDD using ALA was proved to be a procedure with an

KARGER

Fax +41 61 306 12 34
E-Mail karger@karger.ch
www.karger.com

1015–2008/09/0766–0303$26.00/0

Accessible online at:
www.karger.com/pat

Keiji Inoue
Department of Urology
Kochi Medical School
Nankoku, Kochi 783-8505 (Japan)
Tel. +81 88 880 2615, Fax +81 88 880 2404, E-Mail keiji@kochi-u.ac.jp

outstanding sensitivity for detection of superficial bladder cancer, particularly for flat lesions such as dysplasia and carcinoma in situ without additional complication [4–6]. Furthermore, it was suggested that transurethral resection of bladder tumor guided by PDD reduced the risk of residual tumors and subsequent intravesical recurrence compared to conventional transurethral resection of bladder tumor in patients with superficial bladder cancer [7–9].

The principle of PDD was based on tumor specificity of photoactive protoporphyrin IX (PpIX) accumulation. In urothelial cancer (UC), the accumulation of ALA-mediated PpIX was previously reported to be 17 times higher than that in normal mucosa [10]. Since ALA is impermeable through membrane/lipid bilayers [11] and the biosynthesis of heme occurs both in cytosol and mitochondria, the efficacy of ALA-dependent PDD and PDT is restricted by cellular uptake of ALA and/or accumulation of photosensitizer PpIX [12]. Various factors in the mechanism for the preferential accumulation of PpIX in tumor cells have been studied, such as ALA uptake by cells [13, 14], mitochondrial properties [15] and molecules involved in PpIX metabolism including porphobilinogen deaminase [16], ferrochelatase (FC) [17], iron content [18] and transferring receptor [19]. It has been reported that tumor-specific PpIX accumulation is generated by ALA conversion rather than by its initial uptake [20]. However, the mechanism of preferential accumulation of PpIX in UC cells remains obscure.

It is important to clarify the regulatory mechanism of PpIX synthesis mediated by ALA to solve these problems. In the present study, we evaluated the effect of several regulatory factors on PpIX accumulation mediated by ALA in several human UC cell lines. The regulatory factors on PpIX accumulation hereby identified may raise the efficiency of PDD and PDT without requiring an increase in ALA administration.

Materials and Methods

Chemicals

ALA, β-alanine which is an inhibitor of β-transporters of cell membrane, carbonyl cyanide *p*-trifluoromethoxyphenyl hydrazone (FCCP) which is an uncoupler of oxidative phosphorylation in mitochondria, deferoxamine (DFX) which is an iron chelator, tetramethylrhodamine-ethyl-ester (TMRE) which is a potentiometric fluorescent dye for detection of mitochondrial membrane potential, and PpIX were obtained from Sigma Chemical Co. (St. Louis, Mo., USA). NOC-18, a nitric oxide (NO) which is an inhibitor- or FC-generating reagent was obtained from Dojindo Co. Ltd (Kumamoto, Japan). N-methyl protoporphyrin IX (Frontier Scientific) was obtained from Funakosi (Tokyo, Japan). 10-Nonyl acridine orange (NAO) which is a fluorescent dye compound for detection of mitochondria and liposomes was obtained from Molecular Probes (Eugene, Oreg., USA). All other chemicals were of analytical grade and obtained from Nacalai Tesque (Kyoto, Japan). NAO and TMRE were dissolved in DMSO and stored in aliquots at 4°C until use.

Cell Culture

The nontumorigenic human bladder carcinoma cell line 253J-P, the highly tumorigenic and highly metastatic variant 253J B-V isolated from 253J-P and human UC cell line T24 were maintained in Dulbecco's modified Eagle's medium (DMEM) supplemented with 10% fetal bovine serum (FBS; Life Technologies Inc., Carlsbad, Calif., USA) containing 10% FBS with 100 U/ml penicillin and 100 μg/ml streptomycin. Human prostate adenocarcinoma (grade IV) cell line PC-3, a prostate carcinoma cell line DU145 and a renal clear cell adenocarcinoma cell line 786-o, a renal carcinoma A-498 were cultured in DMEM (Invitrogen, Carlsbad, Calif., USA) supplemented with 10% FBS (Equitech Bio, Kerrville, Tex., USA) at 37°C and 5% CO_2. ACHN, a renal cell adenocarcinoma, was cultured in RPMI 1640 supplemented with 10% FBS at 37°C and 5% CO_2. Human renal proximal tubular epithelial cell (RPTEC), as a normal cell line, was maintained in SmBM containing EGF, insulin, hFGF-B, FBS and GA-1000, and REBM containing hydrocortisone, hEGF, FBS, epinephrine, triiodothyronine, transferrin, insulin and GA-1000. Human histiocytic lymphoma U937 as a control malignant cell line, obtained from American Type Culture Collection (Rockville, Md., USA) were maintained in RPMI 1640 medium (Invitrogen) containing 10% FBS with 100 U/ml penicillin and 100 μg/ml streptomycin. Cell cultures were established in 75-cm^2 flasks and kept in a humidified atmosphere with 5% CO_2 at 37°C in accordance with previous reports [21, 22].

Detection of PpIX in Cells Cultured in the Presence of ALA under Fluorescence Microscopy

Cells were seeded in 6-well plates and cultured with serum-free cultured medium containing various concentrations of ALA (0–1 mM) for 0–6 h. The cells were then washed with culture medium and stained with 10 nM NAO for 15 min at 37°C. These cells were washed with PBS and fluorescence of NAO and PpIX was observed by fluorescence microscopy (Axiovert 200; Zeiss, Göttingen, Germany) with a 100-watt halogen lamp. Fluorescence images were made by a highly light-sensitive thermo-electrically cooled charge-coupled device camera (ORCAII-ER; Hamamatsu, Hamamatsu, Japan). The filter combinations used were composed of the following: a 450-nm excitation filter, 510-nm beam splitter and a 515- to 565-nm emission filter for NAO, a fluorescent dye compound for detection of mitochondria and liposomes; a G365-nm excitation filter, an FT580-nm beam splitter and an up LP590-nm emission filter for PpIX; a 488-nm excitation filter, 505-nm beam splitter and a 564-nm emission filter for TMRE, a potentiometric fluorescent dye for detection of mitochondrial membrane potential [23].

Flow Cytometry of Cellular PpIX

All cell lines (4×10^4 cells/ml) were grown on tissue culture plates and were incubated for 24 h. ALA was diluted in RPMI 1640 medium to a stock solution of 1 M, and a final concentration of

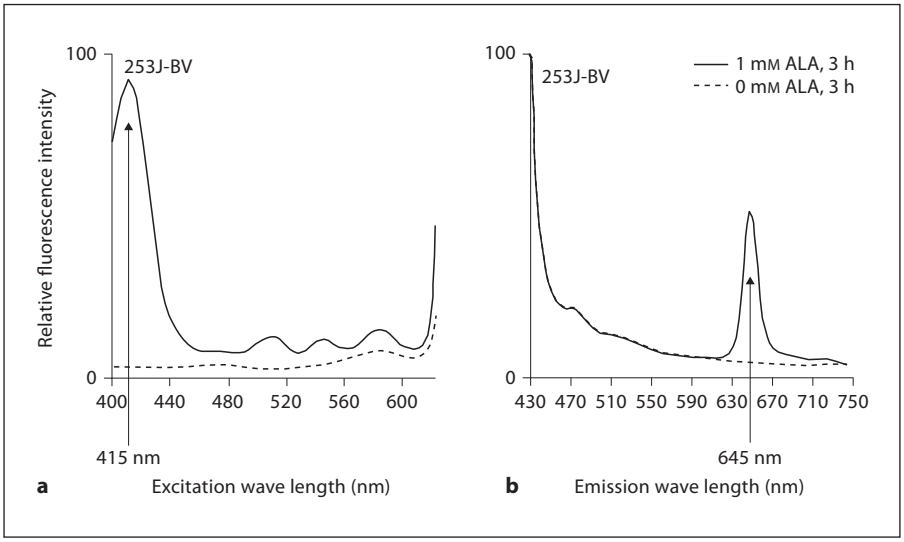

Fig. 1. Excitation and emission spectra of PpIX in ALA-based 253J-BV cells. 253J-BV cells (5×10^5 cells/ml) were incubated with 1 mM ALA for 3 h in FBS-free culture medium at 37°C and obtained the excitation and emission spectra were obtained with a fluorescence spectrophotometer (Hitachi 650-10S). **a** Fluorescence emission spectra of accumulated PpIX in the cells mediated by ALA were obtained by excitation wavelength at 415 nm. **b** Fluorescence excitation spectra of accumulated PpIX in the cells mediated by ALA were obtained at 645-nm emission wavelength. Dotted lines show the curves obtained without ALA.

0.1–1 mM was incubated with cells for 3 h. After incubation with ALA, the cells were washed with PBS (without Ca^{2+} and Mg^{2+}) and scraped off with a rubber policeman. After 10 min of centrifugation at 1,100 rpm, the medium was decanted and 0.5 ml of PBS (without Ca^{2+} and Mg^{2+}) was added. The suspension was measured using a fluorescence-activated cell sorter (FACS Calibur; Becton Dickinson, Mountain View, Calif., USA). Overall, 20,000 cells were measured in each sample (excitation 488 nm, emission 650 nm) [24].

Excitation and Emission Spectra of PpIX in Cells Exposed to ALA

UC cell lines were incubated with 1 mM ALA for 3 h in FBS-free medium. Samples were transferred to a quartz cuvette which was positioned in a spectrofluorometer (Hitachi 650-10S). Excitation for PpIX was 410 nm, and the fluorescence emission was scanned from 400 to 650 nm. Background autofluorescence was determined in cells that had not been incubated with ALA. Emission for PpIX was 645 nm, and the fluorescence excitation was scanned from 430 to 750 nm.

Statistical Analysis

All results are expressed as the mean ± SD, and the significance of differences were by Student's t test (SPSS 11.0 for Windows; SPSS, Tokyo, Japan). $p < 0.05$ were considered significant by Student's t test.

Results

Excitation and Emission Spectra of ALA-Mediated Intracellular PpIX

The absorption spectra of extracted protoporphyrin showed a similar curve to that described by Calzavara-Pinton et al. [25] (data not shown). Excitation and emission spectra of fluorescence in 253J-BV cells incubated with 1 mM ALA for 3 h in the absence of FBS were the same as those of authentic PpIX (Sigma) in the presence of cultured cells (fig. 1a and b). The maximum excitation and emission wavelengths of cells cultured in ALA were 415 and 645 nm, respectively. The excitation wavelength was the same as that of ALA-mediated PpIX in WiDr cells [25]. The levels of PpIX in cells incubated without ALA were below the detection level.

Accumulation of PpIX in ALA-Treated UC Cells (fig. 2)

UC cell lines and U937 cells as a control were incubated with various concentrations and incubation times of ALA. Figure 2 shows the accumulation of cellular PpIX measured by cytometric analysis using FACScan as a function of concentration of added ALA and time of incubation. Figure 2a shows an actual histogram of the analyzed results in 253J-BV cells, and figure 2b shows the ALA concentration-dependent increase in PpIX in UC cell lines and U937 cells as a control. Accumulation of cellular PpIX was linearly increased as a function of added ALA concentration for up to 1 mM. Figure 2c shows the time-dependent ALA-mediated PpIX accumulation after incubation with 1 mM ALA. The time-dependent curves were different between 0.5 and 5 mM of added ALA (data not shown), and a definite lag time was observed in the cells incubated with 0.5 mM ALA. Of the UC cell lines, T24 cell had the strongest potential for dependence on ALA concentration and incubation time in ALA-mediated PpIX synthesis.

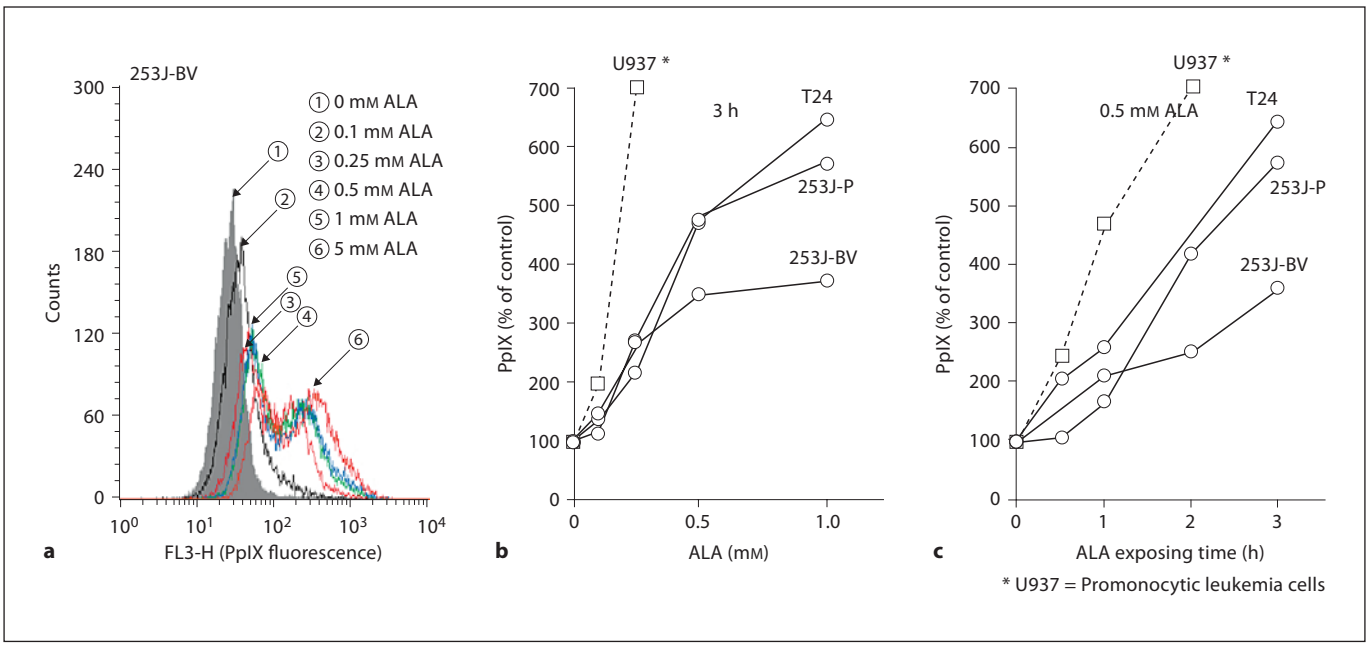

Fig. 2. Accumulation of PpIX in UC cells after incubation with various concentrations of ALA and time of incubation. **a** Cellular content of PpIX was measured by flow cytometry using FACScan FL3-H. **b** Concentration-dependent curve of accumulated PpIX in UC cells and U937 cells after incubation with various concentrations of ALA for 3 h using Cell-Quest (Software version 3.1) by Becton Dickinson. **c** Time dependence curve of accumulated PpIX in UC cells and U937 cells after incubation with 0.5 mM ALA for various times. Similar results were obtained in 3 separate experiments.

Accumulation of PpIX in ALA-Treated Prostate and Kidney Cancer Cells

Figure 3 shows the accumulation of cellular PpIX measured by cytometric analysis using FACScan as a function of concentration of added ALA and time of incubation. Figure 3a and c shows the ALA concentration-dependent increase in PpIX in prostate (fig. 3a) and kidney (fig. 3c) cancer cell lines and U937 cells as a control. Accumulation of cellular PpIX was linearly increased as a function of added ALA concentration for up to 1 mM. Figure 3b and d shows the time-dependent ALA-mediated PpIX accumulation after incubation with 1 mM ALA. The time-dependent curves were different between 0.5 and 5 mM of added ALA (data not shown) and a definite lag time was observed in the cells incubated with 0.5 mM ALA. It was demonstrated that the cancer-specific accumulation of PpIX was dependently increased on ALA concentration and exposure time not only in bladder cancer cell lines but also the cell lines of prostate cancer and renal cancer.

ALA-Mediated PpIX Synthesis in 4 × 10^5 Cells/ml of Various UC Cell Lines

Figure 4 shows the increase rate of PpIX detected by flow cytometer (FACScan) after incubation with 1 mM ALA for 3 h in UC cell lines, T24, 253J-P and 253J-BV compared to RPTEC as a normal cell line and U937 as a control malignant cell line.

The increase rate of PpIX content in UC cell lines [1,483% in T24 ($p = 0.005$), 2,094% in 253J-P ($p = 0.0001$) and 1,454% in 253J-BV ($p = 0.0002$)] and control malignant cell line [1,879% in U937 ($p = 0.0001$)] was significantly 6.5- to 9.4-fold higher compared to that in a normal cell line (222% in RPTEC).

Distribution of ALA-Mediated PpIX in 253J B-V Cells

The subcellular distribution pattern of accumulated ALA-mediated PpIX and mitochondria stained with cardiolipin-specific probe, NAO, and the time courses of the intensity and distribution were studied by fluorescence microscopy (fig. 5).

The intensity of PpIX fluorescence was time-dependently increased in 253J-BV cells after incubation with 1 mM ALA. The granular patterns of the cells were

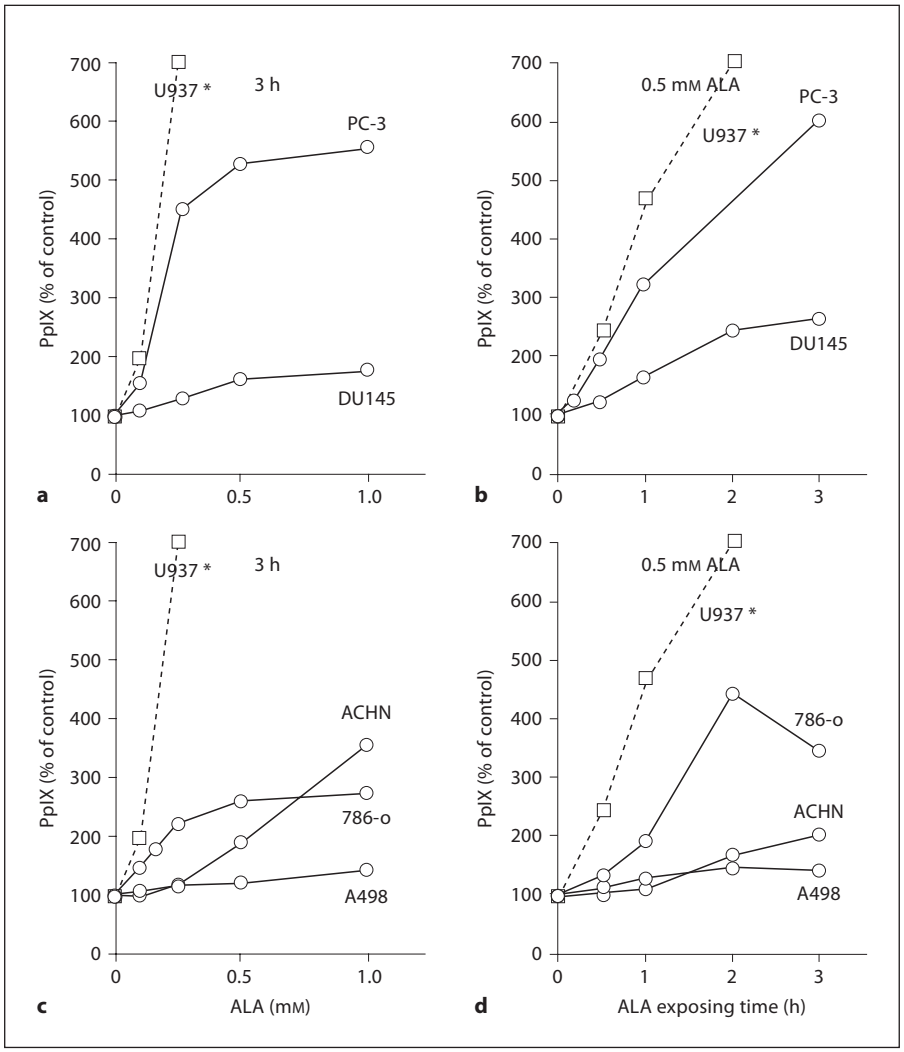

Fig. 3. Accumulation of PpIX in prostate and kidney cancer cells after incubation with various concentrations of ALA and time of incubation. **a** Concentration-dependent curve of accumulated PpIX in prostate cancer cells and U937 cells after incubation with various concentrations of ALA for 3 h using Cell-Quest (Software version 3.1) by Becton Dickinson. **b** Time dependence curve of accumulated PpIX in prostate cancer cells and U937 cells after incubation with 0.5 mM ALA for various times. Similar results were obtained in 3 separate experiments. **c** Concentration-dependent curve of accumulated PpIX in kidney cancer cells and U937 cells after incubation with various concentrations of ALA for 3 h using Cell-Quest (Software version 3.1) by Becton Dickinson. **d** Time dependence curve of accumulated PpIX in kidney cancer cells and U937 cells after incubation with 0.5 mM ALA for various times. Similar results were obtained in 3 separate experiments.

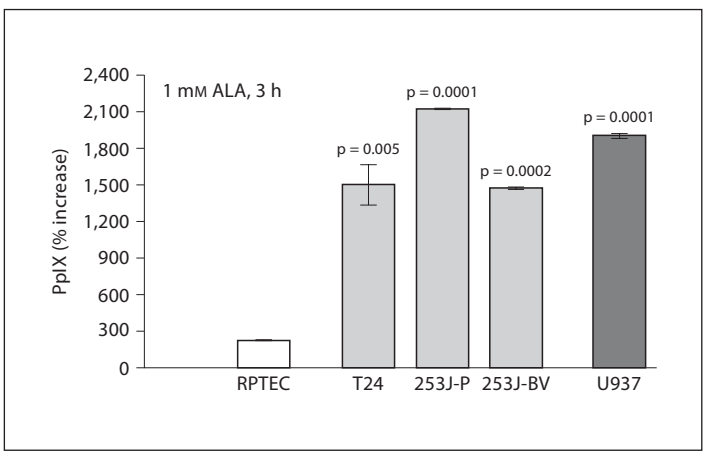

Fig. 4. Accumulation of PpIX in UC cell lines and human bladder smooth muscle cells after incubation with various concentrations of ALA and times of incubation. Experimental conditions were the same as described in figure 2. Figure shows the increase ratio of PpIX in 4×10^5 cells/ml of UC cell lines, human bladder smooth muscle cells, Bd-SMC and human proximal tubular epithelial cells, RPTEC as normal cells, and promonocytic leukemia cells, U-937 as control cell lines after incubation for 3 h with 1 mM ALA.

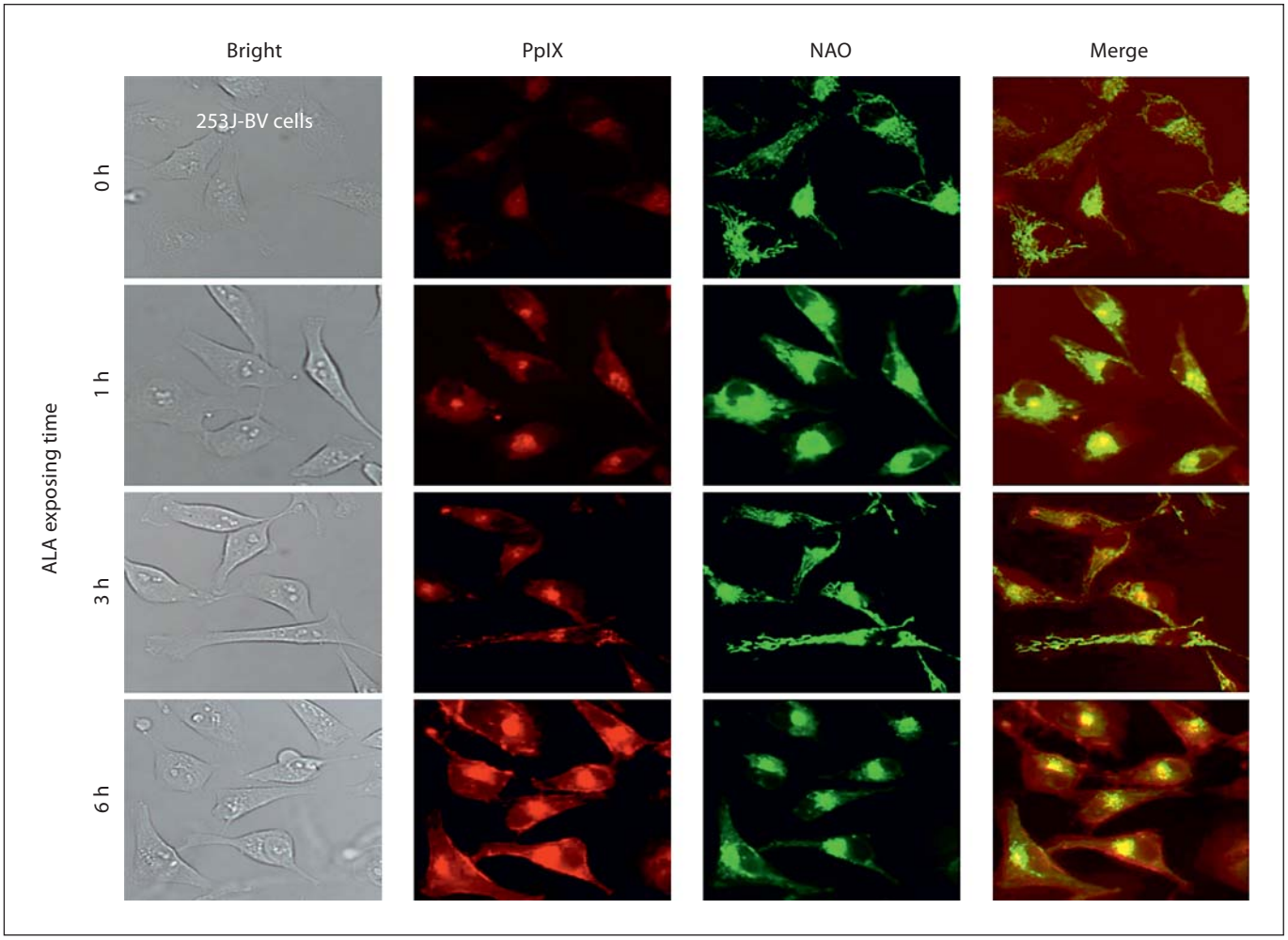

Color version available online

Fig. 5. Intracellular localization of PpIX in 253J-BV cells after incubation with ALA. Experimental conditions were the same as described in figure 2. 253J-BV cells were cultured in the standard medium for various time in the presence of 1 mM ALA. Cells were washed with PBS and stained with 10 nM NAO for 15 min before observation under fluorescence microscopy. Bright and fluorescent indicate the cells observed by microscopy under bright light and fluorescence microscopy using filters of excitation, beam splitter and emission of G365, FT580 and LP590 for PpIX, respectively. Mitochondrial distributions in cells were observed using filters of excitation, beam splitter and emission of 450, 510 and 515–565, respectively. Similar results were obtained in more than 3 separate experiments.

initially similar for both PpIX and NAO, indicating that the distribution of PpIX primarily coincided with mitochondria. However, at later time points, PpIX fluorescence increased in the cytosol, especially in the perinuclear area (data not shown). This was probably due to the diffusion of PpIX from mitochondria to cytosol.

Effect of β-Alanine on the Accumulation of ALA-Mediated PpIX

ALA-induced PpIX accumulation is regulated by various factors including the ALA transport system in the cell membrane. ALA, but not ALA methyl ester, was transported by β-amino acid and GABA carriers in human adenocarcinoma cell line, and the transport was attenuated by 85% in the presence of 10 mM β-alanine, an inhibitor of β-transporters of cell membrane [26, 27]. To elucidate the mechanism of ALA transport in 253J-BV

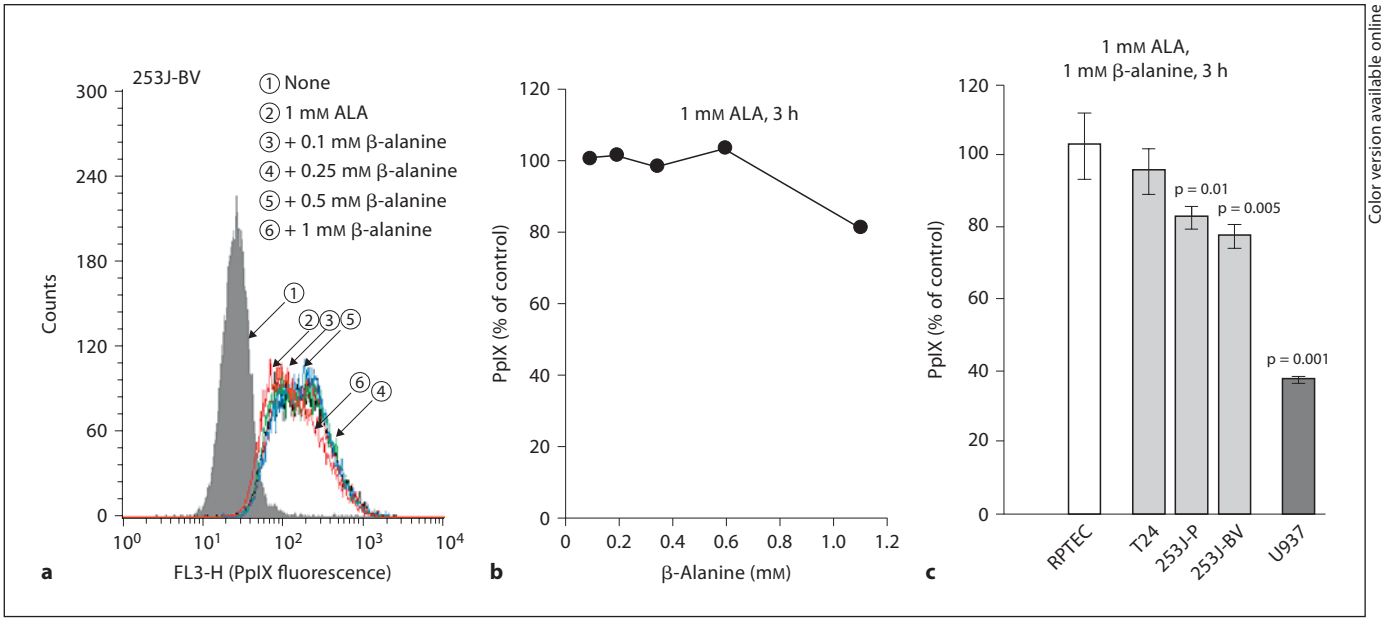

Fig. 6. Concentration-dependent inhibition of ALA-based PpIX accumulation in 253J-BV cells by β-alanine. Experimental conditions were the same as described in figure 2. **a** Concentration-dependent inhibition of PpIX accumulation in 4 × 10^4 cells/ml of 253J-BV cells after incubation with 1 mM ALA for 3 h in the presence of various concentrations of β-alanine. Similar results were obtained in 3 separate experiments. **b** Concentration-dependent inhibition of PpIX accumulation in 4 × 10^4 cells/ml of 253J-BV cells after incubation with 1 mM ALA for 3 h in the presence of various concentrations of β-alanine. Similar results were obtained in 3 separate experiments. **c** Ratio of PpIX accumulation in UC cells and U937 cells compared to control cell lines after incubation with 1 mM ALA for 3 h in the presence of 1 mM β-alanine.

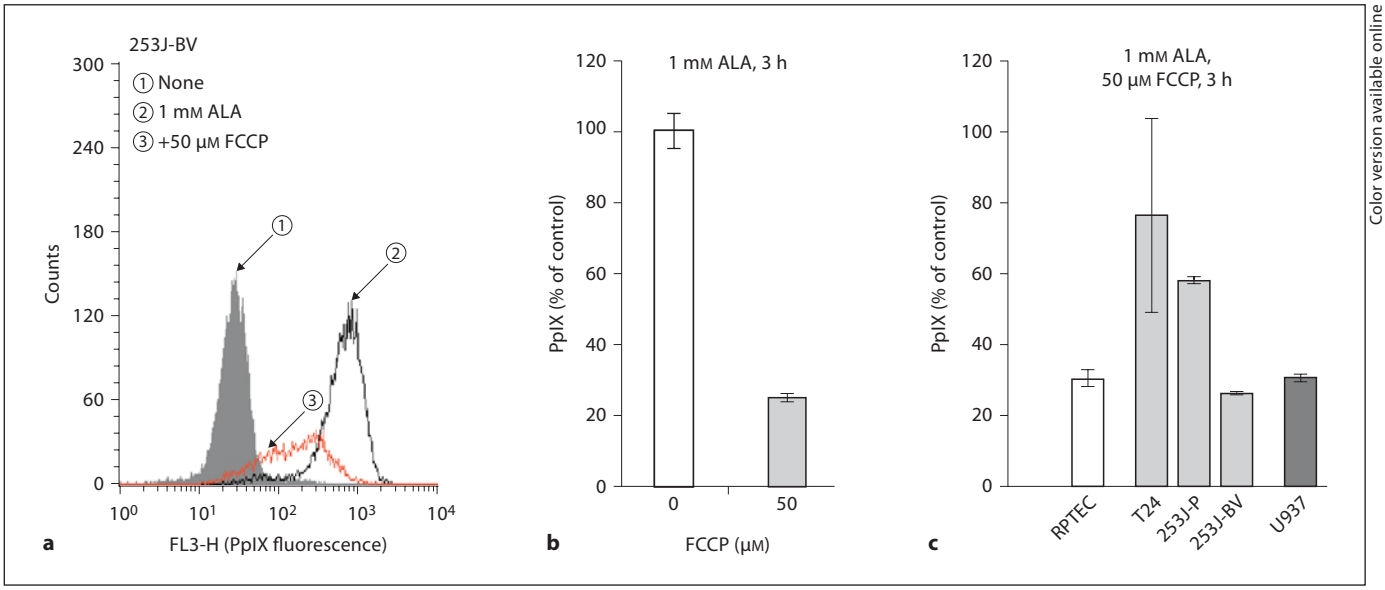

Fig. 7. Concentration-dependent inhibition of ALA-based PpIX accumulation in 253J-BV cells by FCCP. Experimental conditions were the same as described in figure 2. **a** Cellular content of PpIX was measured by flow cytometry using FACScan FL3-H. **b** Concentration-dependent inhibition of PpIX accumulation in 4 × 10^4 cells/ml of 253J-BV cells after incubation with 1 mM ALA for 3 h in the presence or absence of 50 mM FCCP. Similar results were obtained in 3 separate experiments. **c** Ratio of PpIX accumulation in UC cells and U937 cells compared to control cell lines after incubation with 1 mM ALA for 3 h in the presence of 50 μM FCCP.

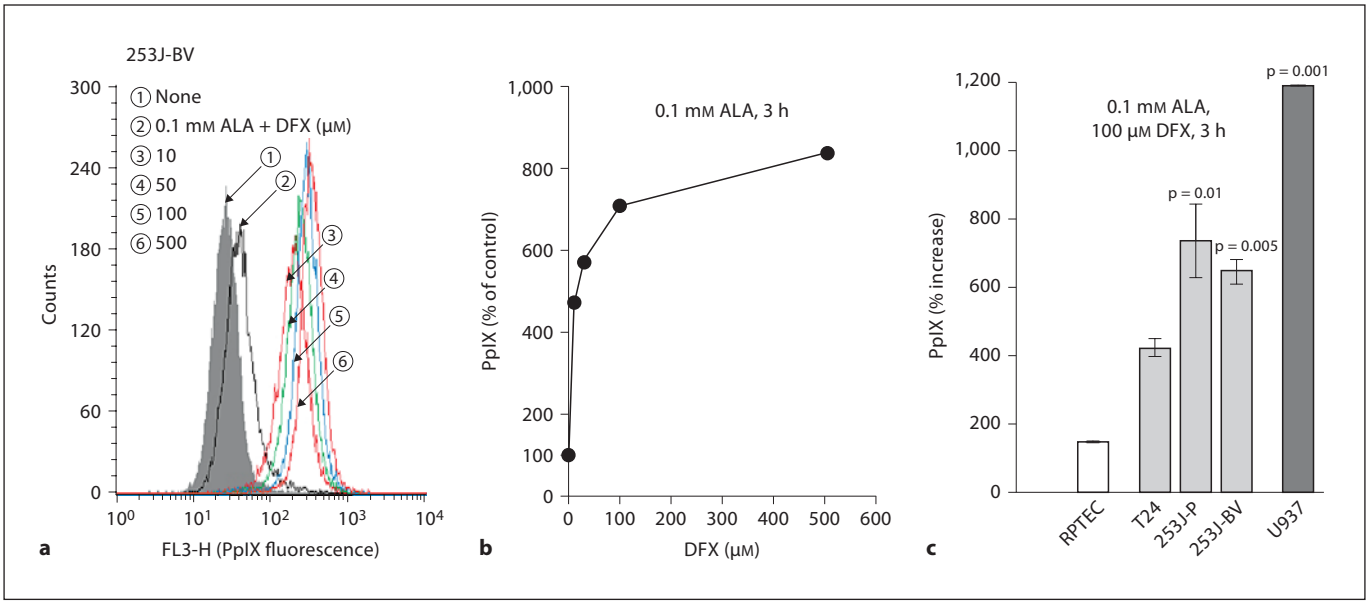

Fig. 8. Concentration-dependent increase in PpIX accumulation in ALA-based 253J-BV cells by DFX. Experimental conditions were the same as described in figure 2. **a** Cellular content of PpIX was measured by flow cytometry using FACScan FL3-H. **b** Concentration-dependent increase in ALA-induced PpIX accumulation in 4 × 10^4 cells/ml of 253J-BV cells after incubation for 3 h with 0.1 mM ALA in the presence of various concentrations of DFX monitored by cytofluorometry. Similar results were obtained in 3 separate experiments. **c** Ratio of PpIX accumulation in UC cells and U937 cells compared to control cell lines after incubation with 0.1 mM ALA for 3 h in the presence of 100 μM DFX.

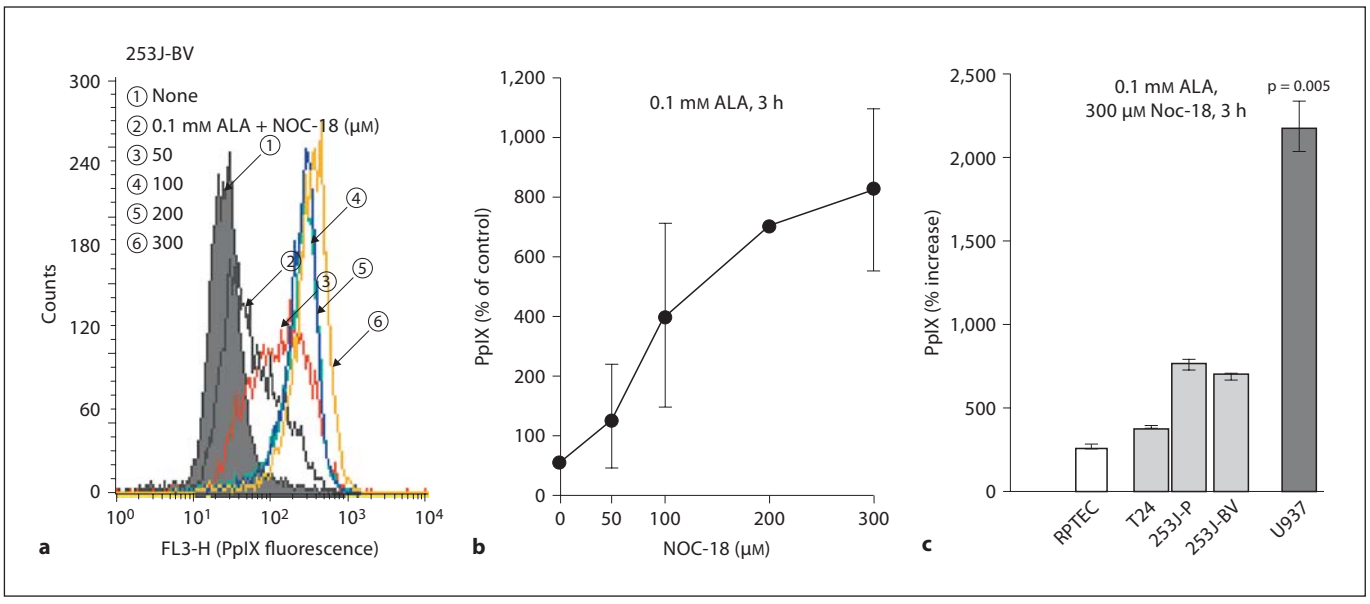

Fig. 9. Concentration-dependent increase in PpIX accumulation in 253J-BV cells incubated with ALA in the presence of NO, NOC-18. Experimental conditions were the same as described in figure 2. **a** Cellular content of PpIX was measured by flow cytometry using FACScan FL3-H. **b** Concentration-dependent increase in ALA-induced PpIX accumulation in 4 × 10^4 cells/ml of 253J-BV cells after incubation for 3 h with 0.1 mM ALA in the presence of various concentrations of NO, NOC-18 monitored by cytofluorometry. Similar results were obtained in 3 separate experiments. **c** Ratio of PpIX accumulation in UC cells and U937 cells compared to control cell lines after incubation with 0.1 mM ALA for 3 h in the presence of 1 μM NOC-18.

cells, the effect of β-alanine on the ALA-mediated accumulation of PpIX was examined.

As shown in figure 6, the ALA-mediated PpIX accumulation was attenuated by β-alanine in a concentration-dependent manner. By the addition of 1 mM β-alanine, ALA-induced PpIX accumulation was significantly attenuated by 23% in 253J B-V ($p = 0.005$), 17% in 253J-P ($p = 0.01$), 5% in T24 ($p > 0.05$) and 63% in U937 ($p = 0.001$; fig. 6).

The result may indicate that a part of the ALA transport in UC cell lines also occurred through BETA transporters.

Effect of FCCP on the Accumulation of ALA-Mediated PpIX

It has been reported that biosynthesis of coproporphyrinogen III from ALA and transport of coprogen into mitochondria occurred via an ATP-dependent process in MLA cells and normal animal cells [15]. Thus, the effect of FCCP, an uncoupler of oxidative phosphorylation in mitochondria, on the ALA-medicated PpIX accumulation was examined to confirm the involvement of the energy requirement reaction.

ALA-mediated PpIX accumulation in the cells was decreased 74% in 253J B-V, 42% in 253J-P, 24% in T24 and 70% in U937 in the presence of 50 μM FCCP (fig. 7). However, there was no statistically significant (all data, $p > 0.05$), because ALA-mediated PpIX accumulation in RPTEC as a normal cell line was also decreased 70% in the presence of 50 μM FCCP (fig. 7).

These results indicate that a part of the ALA-mediated PpIX accumulation in UC cell lines depends on the energy metabolism of these cells. However, the sensitivity to FCCP was different in each cell line.

Effect of DFX on the Accumulation of ALA-Mediated PpIX

FC is the terminal enzyme of the heme-biosynthetic pathway and is thought to be the rate-limiting step for heme production. This pathway required iron, and the heme synthesis was attenuated by low concentration of the iron chelator DFX [28]. Thus, the effect of DFX on the accumulation of ALA-mediated PpIX was examined in UC cell lines.

By the addition of 10–500 μM DFX, the accumulation of ALA-mediated PpIX was strongly increased in UC cell lines but in not normal cells. The accumulation depended on the concentration of DFX (fig. 8). After incubation with 100 μM DFX for 3 h, fluorescence of ALA-mediated PpIX was significantly increased to 6.3-fold of control in 253J-BV ($p = 0.005$), 7.2-fold in 253J-P ($p = 0.01$) and 4.1-fold in T24 ($p > 0.05$), whereas ALA-mediated PpIX accumulation in RPTEC as a normal cell line peaked at 1.4-fold in the presence of 100 μM DFX (fig. 8). This may indicate that the accumulation of ALA-mediated PpIX in UC is a tumor cell-specific reaction.

Effect of FC Inhibitors on the Accumulation of ALA-Mediated PpIX

A similar increase of ALA-mediated PpIX accumulation was also observed by generated nitric oxide (NO), an inhibitor or FC, in transfected inducible-nitric oxide cDNA human embryonic kidney (HEK) 293T cells [29] or in stimulated macrophage cell line RAW 264 [30]. Thus, in this experiment, the effect of NOC-18, an NO-generating reagent, on the PpIX accumulation in ALA-mediated 253J-BV was examined. In the presence of 0.1 mM ALA, NOC-18 (50–300 μM) increased the accumulation of PpIX in UC cell lines [146% in T24 ($p = 0.005$), 299% in 253J-P ($p = 0.0001$) and 274% in 253J-BV ($p = 0.0002$)] in a concentration-dependent manner (fig. 9). However, there was no statistical significance (all data, $p > 0.05$), because ALA-mediated PpIX accumulation in RPTEC peaked at 2.6-fold in the presence of 300 μM NOC-18.

A similar increase in ALA-mediated PpIX accumulation was also induced by manganese ($MnCl_2$), an inhibitor of FC [31]. After 3 h incubation of cells with 1 mM $MnCl_2$ in the presence of 0.1 mM ALA, a more than 1.5-fold increase in PpIX accumulation was observed in 253J-BV, 3.5-fold in 253J-P and 1.7-fold in T24, but not in normal cell lines (data not shown). However, there was no statistical significance (all data, $p > 0.05$) because ALA-mediated PpIX accumulation in RPTEC peaked at 1.2-fold in the presence of 1 mM $MnCl_2$.

These results indicate that the metabolism of accumulated ALA-mediated PpIX to form heme is suppressed by inhibiting FC and iron in these tumors but not in normal cells.

Discussion

The purpose of this study was to clarify the mechanism that regulates the accumulation of ALA-mediated PpIX in human UC cell lines, and to develop an effective method of increasing the PpIX accumulation while minimizing the dose of cytotoxic ALA, leading to improved accuracy in PDD and PDT using ALA. Fluorescence technique as a kinetic analysis revealed that the synthe-

sized endogenous PpIX in ALA-mediated U937 cells localized preferentially in mitochondria and perinuclear regions. The cellular accumulation of PpIX was suppressed by β-alanine, an inhibitor of β-transporters of cell membrane and FCCP, an uncoupler of oxidative phosphorylation in mitochondria. DFX, an iron chelator, $MnCl_2$ and NO (NOC-18), which are contributed to PpIX metabolism by inhibiting FC activity, significantly increased the amount of PpIX in ALA-mediated cancer cells, while minimal enhancement was observed in the normal urothelial cells investigated. These results suggest that ALA-enhanced accumulation of PpIX in UC cells seems to be determined by several steps including de novo synthesis and degradation of synthesized PpIX (fig. 9). Notably, this is the first report to show that the suppression of FC by $MnCl_2$ and NO (NOC-18) in addition to DFX markedly increased PpIX accumulation in UC cells compared to normal cells.

Although the mechanism is not known, it was reported that exogenously administered ALA increased cellular levels of PpIX in most tissues of various organs, and accumulation of PpIX occurred more markedly in tumor cells than in normal cells [12, 20, 32–35]. Especially in the urinary tract, the quantitative analysis of fluorescence spectra showed that PpIX was enhanced 17-fold in urothelial neoplasia compared with normal mucosa [4, 36, 37]. Thus, the physicochemical properties of PpIX have been used for PDD and PDT of patients with tumors [38]. PDD is clinically recognized as an effective detection procedure for various cancers. PDD using ALA in bladder cancer is an officially approved diagnostic procedure in Europe, although many problems concerning the accuracy of diagnosis remain to be solved, such as false fluorescence-positive findings and the photobleaching phenomenon which refers to the reduction of the fluorescence during irradiation. Photoactivation of tissues preferentially kills tumor cells without eliciting severe toxicity to progenitor and stem cells [39]. Although the ALA-dependent PDT has been used successfully in the treatment of oncological and nononcological diseases, the mechanism of this modality remains to be elucidated. Thus, we hope this study marks the first step in clarifying these critical problems.

Previously, to study the mechanism of preferential accumulation of ALA-derived PpIX in malignant cells, several factors have been analyzed, including ALA synthase, a rate-limiting enzyme in heme biosynthesis, cellular uptake of ALA [13, 14, 26, 27], mitochondrial properties [15], key molecules for PpIX metabolism [16, 24], FC activity [17, 29], contents of iron [18, 40] and transferrin receptor [41]. The results of these analyses strongly suggested that the preferential accumulation of ALA-derived PpIX in malignant cells depends on the augmented initial uptake of ALA [17] and the steps of ALA conversion [20] including the activities of PpIX-generating porphobilinogen deaminase [24] and the activity of PpIX-converting FC, a rate-limiting enzyme in heme biosynthesis [29]. Although the activity of FC generally decreases in a variety of tumor cells, inhibition of the enzyme and/or elimination of iron by chelating agents further increased the accumulation of PpIX as described in this study. Furthermore, preliminary experiments in this laboratory revealed that the accumulation of PpIX in primary cultured cells (RPTEC and bladder microvascular endothelial cells, Bd-SMC) with normal FC activity was not affected by a specific inhibitor of the enzyme. Therefore, the results achieved in this study demonstrated that the activity of FC has the most impact on PpIX accumulation in UC cells. In a future study, we will focus on the detailed mechanism of specific PpIX accumulation in cancer cells.

Translocation of synthesized endogenous PpIX from mitochondrial matrix to cytosol also plays an important role in the accumulation of PpIX. A recent report described the localization of ATP-binding cassette (ABC) transporter in mitochondrial membranes that transports synthesized endogenous PpIX into cytosol [42]. Furthermore, Krishnamurthy et al. [43] reported that inhibition of the ABC transporter suppressed the accumulation of PpIX in cells. Thus, mitochondrial ABC transporter may also determine the accumulation of PpIX in tumor cells. This possibility should be studied further.

Stimulation of ALA-mediated accumulation of PpIX by DFX, $MnCl_2$ and NOC-18 suggested that ALA-dependent accumulation of PpIX was enhanced by inhibiting synthesis and/or degradation of heme [44]. Thus, the efficacy of PDD and PDT of malignant tumors could be improved by selectively modulating endogenous synthesis and accumulation of PpIX in tumor. By using regulatory molecules such as DFX and NO, PpIX accumulation was increased while minimizing the dose of ALA, resulting in less cytotoxicity. This is the first such report in UC cells, leading to improved clinical practicability of PDD and PDT.

References

1 Utsuki S, Miyoshi N, Oka H, Miyajima Y, Shimizu S, Suzuki S, Fujii K: Fluorescence-guided resection of metastatic brain tumors using a 5-aminolevulinic acid-induced protoporphyrin IX: pathological study. Brain Tumor Pathol 2007;24:53–55.

2 Braathen LR, Szeimies RM, Basset-Seguin N, Bissonnette R, Foley P, Pariser D, Roelandts R, Wennberg AM, Morton CA, International Society for Photodynamic Therapy in Dermatology: Guidelines on the use of photodynamic therapy for nonmelanoma skin cancer: an international consensus. International Society for Photodynamic Therapy in Dermatology, 2005. J Am Acad Dermatol 2007;56:125–143.

3 May A, Ell C: Diagnosis and treatment of early esophageal cancer. Curr Opin Gastroenterol 2006;22:433–436.

4 Kriegmair M, Baumgartner R, Knuechel R, Steinbach P, Ehsan A, Lumper W, Hofstädter F, Hofstetter A: Fluorescence photodetection of neoplastic urothelial lesions following intravesical instillation of 5-aminolevulinic acid. Urology 1994;44:836–841.

5 Hungerhuber E, Stepp H, Kriegmair M, Stief C, Hofstetter A, Hartmann A, Knuechel R, Karl A, Tritschler S, Zaak D: Seven years' experience with 5-aminolevulinic acid in detection of transitional cell carcinoma of the bladder. Urology 2007;69:260–264.

6 Inoue K, Karashima T, Kamada M, Kurabayashi A, Ohtsuki Y, Shuin T: Clinical experience with intravesical instillations of 5-aminolevulinic acid (5-ALA) for the photodynamic diagnosis using fluorescence cystoscopy for bladder cancer. Nippon Hinyokika Gakkai Zasshi 2006;97:719–729.

7 Filbeck T, Pichlmeier U, Knuechel R, Wieland WF, Roessler W: Clinically relevant improvement of recurrence-free survival with 5-aminolevulinic acid induced fluorescence diagnosis in patients with superficial bladder tumors. J Urol 2002;168:67–71.

8 Filbeck T, Pichlmeier U, Knuechel R, Wieland WF, Roessler W: Reducing the risk of superficial bladder cancer recurrence with 5-aminolevulinic acid-induced fluorescence diagnosis. Results of a 5-year study. Urologe A 2003;42:1366–1373.

9 Denzinger S, Burger M, Walter B, Knuechel R, Roessler W, Wieland WF, Filbeck T: Clinically relevant reduction in risk of recurrence of superficial bladder cancer using 5-aminolevulinic acid-induced fluorescence diagnosis: 8-year results of prospective randomized study. Urology 2007;69:675–679.

10 Filbeck T, Pichlmeier U, Knuechel R, Wieland WF, Roessler W: Do patients profit from 5-aminolevulinic acid-induced fluorescence diagnosis in transurethral resection of bladder carcinoma? Urology 2002;60:1025–1028.

11 Lopez RF, Lange N, Guy R, Bentley MV: Photodynamic therapy of skin cancer: controlled drug delivery of 5-ALA and its esters. Adv Drug Deliv 2004;56:77–94.

12 Kelty CJ, Brown NJ, Reed MW, Ackroyd R: The use of 5-aminolaevulinic acid as a photosensitiser in photodynamic therapy and photodiagnosis. Photochem Photobiol Sci 2002;1:158–168.

13 Döring F, Walter J, Will J, Focking M, Boll M, Amasheh S, Clauss W, Daniel H: Delta-aminolevulinic acid transport by intestinal and renal peptide transporters and its physiological and clinical implications. J Clin Invest 1998;101:2761–2767.

14 Rud E, Gederaas O, Hogset A, Berg K: 5-aminolevulinic acid, but not 5-aminolevulinic acid esters, is transported into adenocarcinoma cells by system BETA transporters. Photochem Photobiol 2000;71:640–647.

15 Rebeiz N, Arkins S, Kelley KW, Rebeiz CA. Enhancement of coproporphyrinogen III transport into isolated transformed leukocyte mitochondria by ATP. Arch Biochem Biophys 1996;333:475–481.

16 Hinnen P, de Rooij FW, Terlouw EM, Edixhoven A, van Dekken H, van Hillegersberg R, Tilanus HW, Wilson JH, Siersema PD: Porphyrin biosynthesis in human Barrett's oesophagus and adenocarcinoma after ingestion of 5-aminolaevulinic acid. Br J Cancer 2000;83:539–543.

17 Ohgari Y, Nakayasu Y, Kitajima S, Sawamoto M, Mori H, Shimokawa O, Matsui H, Taketani S: Mechanisms involved in delta-aminolevulinic acid (ALA)-induced photosensitivity of tumor cells: relation of ferrochelatase and uptake of ALA to the accumulation of protoporphyrin. Biochem Pharmacol 2005;71:42–49.

18 Krieg RC, Fickweiler S, Wolfbeis OS, Knuechel R: Cell-type specific protoporphyrin IX metabolism in human bladder cancer in vitro. Photochem Photobiol 2000;72:226–233.

19 Piccinelli P, Samuelsson T: Evolution of the iron-responsive element. RNA 2007;13:952–966.

20 Krieg RC, Messmann H, Rauch J, Seeger S, Knuechel R: Metabolic characterization of tumor cell-specific protoporphyrin IX accumulation after exposure to 5-aminolevulinic acid in human colonic cells. Photochem Photobiol 2002;76:518–525.

21 Dinney CP, Fishbeck R, Singh RK, Eve B, Pathak S, Brown N, Xie B, Fan D, Bucana CD, Fidler IJ, Killion JJ: Isolation and characterization of metastatic variants from human transitional cell carcinoma passaged by orthotopic implantation in athymic nude mice. J Urol 1995;154:1532–1538.

22 Fujita H, Utsumi T, Muranaka S, Ogino T, Yano H, Akiyama J, Yasuda T, Utsumi K: Involvement of Ras/extracellular signal-regulated kinase, but not Akt pathway in risedronate-induced apoptosis of U937 cells and its suppression by cytochalasin B. Biochem Pharmacol 2005;69:1773–1784.

23 Ji Z, Yang G, Vasovic V, Cunderlikova B, Suo Z, Nesland JM, Peng Q: Subcellular localization pattern of protoporphyrin IX is an important determinant or its photodynamic efficiency of human carcinoma and normal cell lines. J Photochem Photobiol B 2006;84:213–220.

24 Hirai K, Sasahira T, Ohmori H, Fujii K, Kuniyasu H: Inhibition of heme oxygenase-1 by zinc protoporphyrin IX reduces tumor growth of LL/2 lung cancer in C57BL mice. Int J Cancer 2007;120:500–505.

25 Calzavara-Pinton PG, Venturini M, Sala R: Photodynamic therapy: update 2006. Part 1: photochemistry and photobiology. J Eur Acad Dermatol Venereol 2007;21:293–302.

26 Rud E, Gederaas O, Hogset A, Berg K: 5-aminolevulinic acid, but not 5-aminolevulinic acid esters, is transported into adenocarcinoma cells by system BETA transporters. Photochem Photobiol 2006;71:640–647.

27 Rodriguez L, Batlle A, Di Venosa G, Battah S, Dobbin P, Macrobert AJ, Casas A: Mechanisms of 5-aminolevulinic acid ester uptake in mammalian cells. Br J Pharmacol 2006;147:825–833.

28 Juzenas P, Juzeniene A, Moan J: Deferoxamine photosensitizes cancer cells in vitro. Biochem Biophys Res Commun 2005;332:388–391.

29 Fadigan A, Dailey HA: Inhibition of ferrochelatase during differentiation of murine erythroleukaemia cells. Biochem J 1987;243:419–424.

30 Furukawa T, Adachi Y, Fujisawa J, Kambe T, Yamaguchi-Iwai Y, Sasaki R, Kuwahara J, Ikehara S, Tokunaga R, Taketani S: Involvement of PLAGL2 in activation of iron deficient- and hypoxia-induced gene expression in mouse cell lines. Oncogene 2001;20:4718–4727.

31 Yamamoto F, Ohgari Y, Yamaki N, Kitajima S, Shimokawa O, Matsui H, Taketani S: The role of nitric oxide in delta-aminolevulinic acid (ALA)-induced photosensitivity of cancerous cells. Biochem Biophys Res Commun 2007;353:541–546.

32 Datta SN, Loh CS, MacRobert AJ, Whatley SD, Matthews PN: Quantitative studies of the kinetics of 5-aminolaevulinic acid-induced fluorescence in bladder transitional cell carcinoma. Br J Cancer 1998;78:1113–1118.

33 Navone NM, Polo CF, Frisardi AL, Andrade NE, Battle AM: Heme biosynthesis in human breast cancer-mimetic 'in vitro' studies and some heme enzymic activity levels. Int J Biochem 1990;22:1407–1411.

34 Hinnen P, de Rooij FW, van Velthuysen ML, Edixhoven A, van Hillegersberg R, Tilanus HW, Wilson JH, Siersema PD: Biochemical basis of 5-aminolaevulinic acid-induced protoporphyrin IX accumulation: a study in patients with (pre)malignant lesions of the oesophagus. Br J Cancer 1998;78:679–682.
35 Bartosova J, Hrkal Z: Accumulation of protoporphyrin-IX (PpIX) in leukemic cell lines following induction by 5-aminolevulinic acid (ALA). Comp Biochem Physiol C Toxicol Pharmacol 2000;126:245–252.
36 Steinbach P, Weingandt H, Baumgartner R, Kriegmair M, Hofstädter F, Knüchel R: Cellular fluorescence of the endogenous photosensitizer protoporphyrin IX following exposure to 5-aminolevulinic acid. Photochem Photobiol 1995;62:887–895.
37 Kriegmair M, Baumgartner R, Knuechel R, Steinbach P, Ehsan A, Lumper W, Hofstädter F, Hofstetter A: Fluorescence photodetection of neoplastic urothelial lesions following intravesical instillation of 5-aminolevulinic acid. Urology 1994;44:836–841.
38 Collaud S, Juzeniene A, Moan J, Lange N: On the selectivity of 5-aminolevulinic acid-induced protoporphyrin IX formation. Curr Med Chem Anticancer Agents 2004;4:301–316.
39 Sharman WM, van Lier JE, Allen CM: Targeted photodynamic therapy via receptor mediated delivery systems. Adv Drug Deliv Rev 2004;56:53–76.
40 Inoue A, Muranaka S, Fujita H, Kanno T, Tamai H, Utsumi K: Molecular mechanism of diclofenac-induced apoptosis of promyelocytic leukemia: dependency on reactive oxygen species, Akt, Bid, cytochrome and caspase pathway. Free Radic Biol Med 2004;37:1290–1299.
41 Piccinelli P, Samuelsson T: Evolution of the iron-responsive element. RNA 2007;13:952–966.
42 Kabe Y, Ohmori M, Shinouchi K, Tsuboi Y, Hirao S, Azuma M, Watanabe H, Okura I, Handa H: Porphyrin accumulation in mitochondria is mediated by 2-oxoglutarate carrier. J Biol Chem 2006;281:31729–31735.
43 Krishnamurthy P, Xie T, Schuetz JD: The role of transporters in cellular heme and porphyrin homeostasis. Pharmacol Ther 2007;114:345–358.
44 Liu Y, Zhu B, Luo L, Li P, Paty DW, Cynader MS: Heme oxygenase-1 plays an important protective role in experimental autoimmune encephalomyelitis. Neuroreport 2001;12:1841–1845.